Resonantly pumped 1.645 μm high repetition rate Er:YAG laser Q-switched by a graphene as a saturable absorber

Chunqing Gao,[1,*] Ran Wang,[1] Lingni Zhu,[1] Mingwei Gao,[1] Qing Wang,[2] Zhiguo Zhang,[2] Zhiyi Wei,[2] Jingjing Lin,[3] and Liwei Guo[3]

[1]*School of Opto-Electronics, Beijing Institute of Technology, Beijing 100081, China*

[2]*Laboratory of Optical Physics, Beijing National Laboratory for Condensed Matter Physics, Institute of Physics, Chinese Academy of Sciences, Beijing 100190, China*

[3]*Research & Development Center for Functional Crystals, Beijing National Laboratory for Condensed Matter Physics, Institute of Physics, Chinese Academy of Sciences, Beijing 100190, China*

**Corresponding author: gao@bit.edu.cn*

Received September 23, 2011; revised January 5, 2012; accepted January 6, 2012; posted January 9, 2012 (Doc. ID 154669); published February 10, 2012

A fiber laser resonantly pumped 1.645 μm passively Q-switched Er:YAG laser is reported. Graphene on a silicon carbide was used as the saturable absorber for the Q-switching. The pulse energy of the 1.645 μm Q-switched Er:YAG laser was 7.05 μJ, with a pulse repetition rate of 35.6 kHz and an average output power of 251 mW. © 2012 Optical Society of America

OCIS codes: 140.3540, 140.3580, 140.3500.

Q-switched solid-state lasers operating in the eye-safe wavelength regime around 1.6 μm have important applications in Doppler wind lidars, differential absorption lidars, ranging, and optical communication [1–3]. In recent years, passively Q-switched Er:YAG lasers operating at 1.6 μm have attracted a great deal of attention. Robert D. Stultz *et al.* demonstrated a Cr:ZnSe passively Q-switched Er:YAG laser at 1.617 μm in 2005 [3]. In 2008 Igor S. Moskalev *et al.* used the Cr:ZnSe saturable absorber and a narrow-band volumetric Bragg grating to generate a passively Q-switched 1.645 μm Er:YAG laser [4]. Recently graphene has been paid great attention and has been identified as a potential material of the saturable absorber for Q-switched lasers [5–9]. Q. L. Bao *et al.* reported that graphene has a much lower saturation intensity [10,11], larger saturable-absorption modulation depth [8], higher damage threshold [12,13], ultrafast recovery time, and an ultrabroad wavelength-independent saturable-absorption range (300–2500 nm) [13]. Therefore, unlike conventional saturable absorbers (Cr:YAG, SESAM, Cr:ZnSe, GaAs, etc.), the graphene is suitable for many lasers at different wavelengths. Using the graphene as a passive Q-switcher, H. Zhang *et al.* first demonstrated a mode-locked erbium-doped fiber laser in 2009 with single pulse energy of 7.5 nJ and pulse width of 415 fs [12]. In 2011 Q. Wang *et al.* reported a 1.064 μm Nd:YVO4 laser passively Q-switched by using a few-layer graphene. The average output power was 575 mW at 1.064 μm, with pulse energy of 0.68 μJ and a pulse repetition rate of 850 kHz [7]. In 2011 H. H. Yu *et al.* reported a 1.064 μm Nd:LuVO$_4$ laser passively Q-switched by a graphene. The average output power was 474 mW, with pulse energy of 0.6 μJ and a pulse repetition frequency of 795 kHz [14]. To the best of our knowledge, there is no report on the 1.6 μm Q-switched lasers passively Q-switched by the graphene. This Letter first reported a resonantly pumped 1645 nm Q-switched Er:YAG laser by using a few-layer graphene on SiC as a passive saturable absorber.

The schematic of the experimental setup of the resonantly pumped passively Q-switched Er:YAG laser is shown in Fig. 1. The pump source was an Er,Yb fiber laser with a center wavelength of 1.532 μm. The spectral width of the pumping fiber was 0.2 nm (FWHM). The advantage of the resonantly pumping is to reduce the heat effect of the quasi-three-level Er:YAG crystal and enable better laser efficiency. The laser medium was an Er:YAG crystal with a diameter of 4 mm and a length of 30 mm. The Er doped concentration of the Er:YAG crystal was 0.5 at%. Two surfaces of the Er:YAG crystal were coated with high transmission coating at 1.6 μm ($T > 99.9\%$) and high transmission coating at 1.5 μm ($T > 95\%$), respectively. The pumping beam was focused by coupling optics into the Er:YAG crystal. The radius of the pump beam in the Er:YAG crystal was less than 300 μm.

A *L*-shaped concave-plane resonator was designed for the Q-switched Er:YAG laser. The concave mirror had a radius of curvature of 200 mm, and was coated with an antireflection coating at 1.532 μm and a high reflection coating at 1.645 μm. The output coupler was a plane plate and had a transmittance of 10% at 1.645 μm. For obtaining passive Q-switching of the Er:YAG laser, a graphene saturable absorber was inserted into the resonator close to the output coupler. The graphene was epitaxially

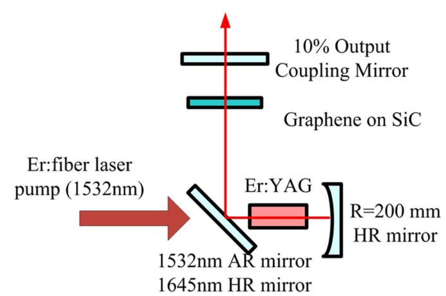

Fig. 1. (Color online) Experimental setup of a resonantly pumped 1.645 μm *L*-shaped Er:YAG laser.

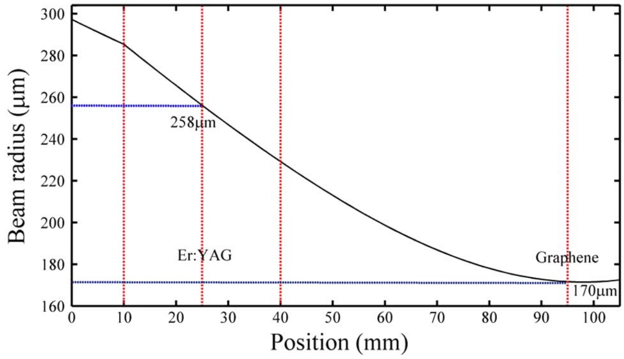

Fig. 2. (Color online) Beam radii of the 1.645 μm Q-switched Er:YAG laser inside the resonator.

grown on SiC with an aperture size of 4×4 mm^2. The thickness of the graphene was estimated to be less than two layers, which was quasimonolayer [7]. To avoid the feedback caused by the reflectance of the pumping beam, the resonator of the Er:YAG laser was deliberately but only slightly misaligned with respect to the pumping beam. The advantage of the L-shaped resonator was to prevent the pumping beam from affecting the graphene saturable absorber. The total resonator length was approximately 115 mm. The beam radius of the Er:YAG laser inside the resonator was calculated by using the software MATLAB. Figure 2 shows the simulated result. In the middle of the Er:YAG crystal, the radius of the oscillating mode was about 258 μm, and the radius of the oscillating mode on the graphene on SiC was about 170 μm. The Er:YAG crystal was mounted in a copper heat sink, and the temperature of the heat sink was controlled at 18 °C by using a semiconductor thermal electric cooler.

In the experiment, we first studied the CW operation of the 1.645 μm Er:YAG laser. When the incident pump power was 6.8 W, the CW 1645 nm Er:YAG laser yielded an output power of 850 mW. In respect to the incident pump power the slope efficiency of the Er:YAG laser was 25.6%. Then graphene on SiC was inserted into the resonator for Q-switching. In the Q-switched mode, the threshold pumping power increased to 4.5 W. The average output power was 251 mW when the incident pump power was 6.8 W. The slope efficiency of the Q-switched Er:YAG laser was 9.4%. Since the uncoated surface of the graphene on SiC has a reflection of about 20%, the intracavity loss of the Er:YAG laser increased. So the average output power and the efficiency of the Q-switched Er:YAG laser were lower than that in the CW mode. Figure 3 shows output powers in the CW mode and in the passively Q-switched mode with respect to pump powers of the Er,Yb fiber laser.

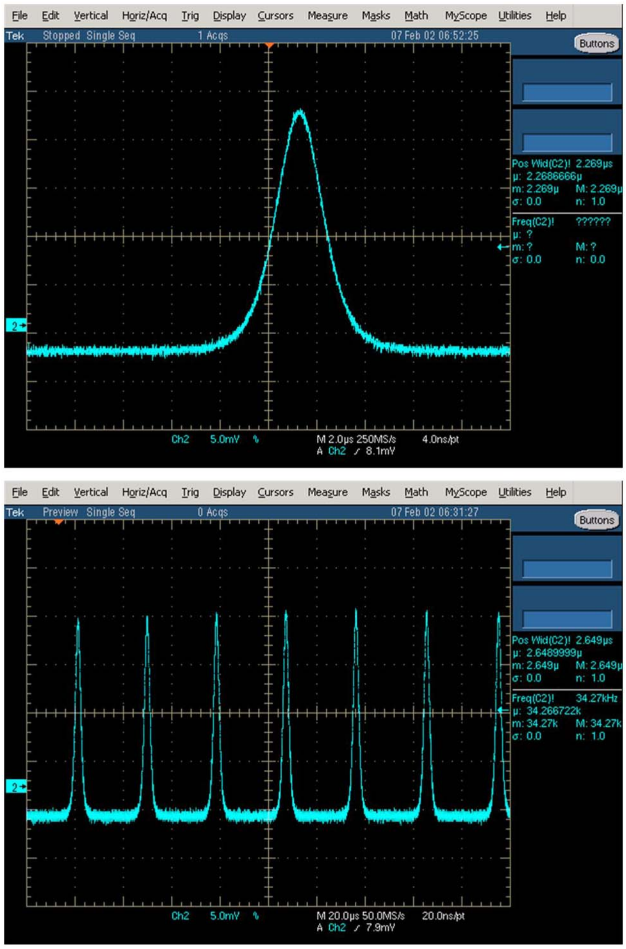

Fig. 4. (Color online) Pulse profiles of the Q-switched Er:YAG laser when the pulse repetition rate was 35.6 kHz. Top: Single output pulse of the passively Q-switched Er:YAG laser. Bottom: Pulse train of the passively Q-switched Er:YAG laser.

The temporal behavior of the 1.645 μm Q-switched pulse was recorded in a digital oscilloscope. Adjusting the Q-switcher and shifting the SiC to allow the laser

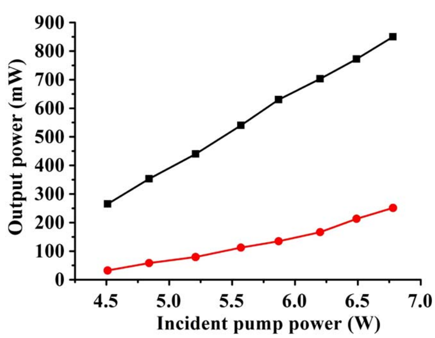

Fig. 3. (Color online) Output power as function of pump power of Er:YAG laser with (■) and without (•) graphene.

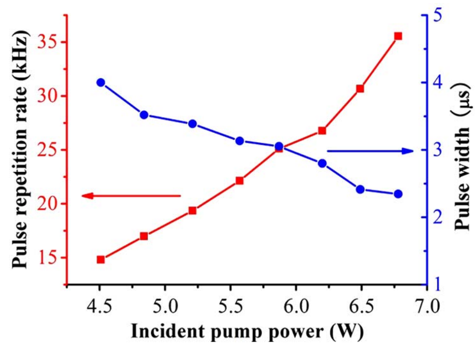

Fig. 5. (Color online) Pulse repetition rate and pulse width with the increase of incident pump power for Q-switching operation ■ pulse repetition rate • pulse width.

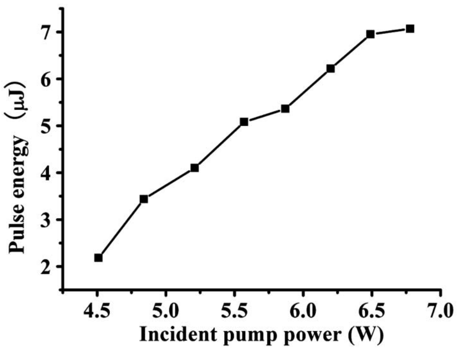

Fig. 6. Pulse energy versus the incident pump power for the Q-switched mode.

incident on an ideal spot, we obtained a stable Q-switched Er:YAG laser. Figure 4 (top) shows the pulse profile of the Q-switched Er:YAG laser performed with a subnanosecond optical detector at the highest pump power of 6.8 W. Figure 4 (bottom) shows the pulse train of the Q-switching.

The pulse repetition rate and pulse width with respect to the incident pump power for the Q-switched operation are shown in Fig. 5. The pulse width was 4 μs near the threshold and decreased almost linearly to 2.34 μs at the maximum incident pump power of 6.8 W, while the pulse repetition rate scaled proportionately with the pump power above lasing threshold. Figure 6 shows the Q-switched pulse energy with respect to the incident pump power. At an incident pump power of 6.8 W, the Q-switched pulse repetition rate reached 35.6 kHz and the pulse energy reached 7.05 μJ. The Q-switched pulse energy increased when the incident pump power increased.

In summary, an Er,Yb fiber laser pumped 1.645 μm passively Q-switched Er:YAG laser was demonstrated. The maximum output power was 251 mW, with pulse energy of 7.05 μJ and a pulse repetition rate of 35.6 kHz. To our knowledge, this is the highest pulse repetition rate Q-switched Er:YAG laser and is also the first use of a graphene saturable absorber as a passive Q-switcher for 1.6 μm Er:YAG lasers.

This work is partly supported by the National Natural Science Foundation of China (NSFC) (61178027), the Doctoral Fund of Ministry of Education of China (20101101110015), and the National Basic Research Program of China (2011CB932700).

References

1. W. J. Kim, D. Y. Shen, J. K. Sahu, and W. A. Clarkson, Opt. Express **16**, 5807 (2008).
2. M. Němeca, H. Jelínkováa, J. Šulca, K. Nejezchlebb, and V. Škodab, Proc. SPIE **7721**, 772113 (2010).
3. R. D. Stultz, V. Leyva, and K. Spariosu, Appl. Phys. Lett. **87**, 241118 (2005).
4. I. S. Moskalev, V. V. Fedorov, V. P. Gapontsev, D. V. Gapontsev, N. S. Platonov, and S. B. Mirov, Opt. Express **16**, 19429 (2008).
5. F. Bonaccorso, Z. Sun, T. Hasan, and A. C. Ferrari, Nat. Photon. **4**, 611 (2010).
6. Z. Q. Luo, M. Zhou, J. Weng, G. M. Huang, H. Y. Xu, C. C. Ye, and Z. P. Cai, Opt. Lett **35**, 3709 (2010).
7. Q. Wang, Z. Y. Wei, J. J. Lin, Y. D. Zhang, L. W. Guo, and Z. G. Zhang, in Advances in Optical Materials, OSA Technical Digest (CD) (Optical Society of America, 2011), paper AIThF3.
8. M. Liu, X. B. Yin, E. Ulin-Avila, B. S. Geng, T. Zentgraf, L. Ju, F. Wang, and X. Zhang, Nature **474**, 64 (2011).
9. L. Liao, Y.-C. Lin, M. Bao, R. Cheng, J. Bai, Y. Liu, Y. Qu, K. L. Wang, Y. Huang, and X. Duan, Nature **467**, 305 (2010).
10. Q. L. Bao, H. Zhang, Y. Wang, Z. H. Ni, Y. L. Yan, Z. X. Shen, K. P. Loh, and D. Y. Tang, Adv. Funct. Mater. **19**, 3077 (2009).
11. H. Zhang, Q. L. Bao, D. Y. Tang, L. M. Zhao, and K. P. Loh, Appl. Phys. Lett. **95**, 141103 (2009).
12. H. Zhang, D. Y. Tang, L. M. Zhao, Q. L. Bao, and K. P. Loh, Opt. Express **17**, 017630 (2009).
13. W. D. Tan, C. Y. Su, R. J. Knize, G. Q. Xie, L. J. Li, and D. Y. Tang, Appl. Phys. Lett. **96**, 031106 (2010).
14. H. H. Yu, X. F. Chen, X. B. Hu, S. D. Zhuang, Z. P. Wang, X. G. Xu, J. Y. Wang, H. J. Zhang, and M. H. Jiang, Appl. Phys. Express **4**, 022704 (2011).